SERI/TP-253-2819
UC Category: 62a
DE85016885

System Performance Analysis of Stretched Membrane Heliostats

J.V. Anderson
L.M. Murphy
W. Short
T. Wendelin

December 1985

Prepared for the ASME Solar
Division Annual Conference
Anaheim, California
14-17 April 1986

Prepared under Task No. 5112.31
FTP No. 510

Solar Energy Research Institute
A Division of Midwest Research Institute

1617 Cole Boulevard
Golden, Colorado 80401

Prepared for the
U.S. Department of Energy
Contract No. DE-AC02-83CH10093

Printed in the United States of America
Available from:
National Technical Information Service
U.S. Department of Commerce
5285 Port Royal Road
Springfield, VA 22161

Price: Microfiche A01
Printed Copy A02

Codes are used for pricing all publications. The code is determined by the number of pages in the publication. Information pertaining to the pricing codes can be found in the current issue of the following publications, which are generally available in most libraries: *Energy Research Abstracts, (ERA); Government Reports Announcements* and Index (*GRA* and I); *Scientific and Technical Abstract Reports (STAR);* and publication, NTIS-PR-360 available from NTIS at the above address.

SYSTEM PERFORMANCE ANALYSIS OF STRETCHED MEMBRANE HELIOSTATS

J. V. Anderson
L. M. Murphy
W. Short
T. Wendelin

Solar Energy Research Institute
Golden, Colorado

ABSTRACT

The optical performance of both focused and unfocused stretched membrane heliostats was examined in the context of the overall cost and performance of central receiver systems. The sensitivity of optical performance to variations in design parameters such as the system size (capacity), delivery temperature, heliostat size, and heliostat surface quality was also examined. The results support the conclusion that focused stretched membrane systems provide an economically attractive alternative to current glass/metal heliostats over essentially the entire range of design parameters studied. In addition, unfocused stretched membrane heliostats may be attractive for a somewhat more limited range of applications, which would include the larger plant sizes (e.g., 450 MW_{th}) and lower delivery temperatures (e.g., 450°C), or situations in which the heliostat size could economically be reduced.

INTRODUCTION

Heliostat costs have long been recognized as a major factor in the cost of solar central receiver plants. Research on stretched membrane heliostats has been emphasized for some time because of their potential as a cost-effective alternative to the glass/metal designs currently available. However, the cost and performance potential of stretched membrane heliostats from a system perspective has not been studied until this time.

The purpose of this study is to examine both the cost and the performance of stretched membrane heliostats relative to those of current generation glass/metal heliostats in the context of the total system cost and performance. The study examines the sensitivity of the relative performance and cost of fields of heliostats to a number of parameter variations for both focused and unfocused stretched membrane modules. The parameters examined included the plant size (75 MW and 450 MW), delivery temperature (450°C to 1050°C), and heliostat module size (25 m^2, 50 m^2, and 100 m^2). In addition, we varied a number of parameters related to the quality of the reflective surface. These included the specularity,[1] the hemispherical reflectance, and the macroscopic surface normal errors.

Stretched membrane heliostats normally consist of a thin, high-strength structural membrane, usually of steel or aluminum, stretched over a circular supporting ring. This structural membrane is covered by a reflective film, typically a metalized polymer material. Both focused and unfocused heliostats are assumed to be of double membrane construction, where two parallel membranes are attached to the planar faces of the ring. Focusing is achieved by drawing a partial vacuum in the plenum between the two membranes to draw the reflector surface into the desired shape.

GROUND RULES AND ASSUMPTIONS

The ground rules and assumptions used in this study are listed below.

Heliostats

We used state-of-the-art, 100-m^2 glass/metal heliostats as the baseline standard of comparison. Each heliostat has 2-x-6-ft mirror panels arranged in a twelve-panel array focused in two directions and canted on-axis.

We studied focused and unfocused stretched membrane heliostats using the double membrane construction, and sized them at 25 m^2, 50 m^2, and 100 m^2. We assumed that the focused stretched membrane heliostats used the vacuum/pressure active control of the reflector surface proposed by Sandia National Laboratories, Livermore (SNLL). All deformations in the unfocused stretched membrane heliostats were measured relative to a perfectly flat reference plane.

We have used standard, documented (2) approaches in considering reflector surface error effects. Specifically, we assumed that specular reflectivity can be represented as the product of two independent functions: the total hemispherical reflectivity and a statistical geometric function that describes the broadening of the scattered reflective beam. We con-

[1] Specularity refers to the degree of spreading of the reflected beam about the specular direction.

sidered independent variations in both of these parameters.

Both the specularity loss (which is a microscopic surface effect) and the macroscopic surface slope errors contribute to the broadening of the reflected beam from a heliostat surface. The specularity losses arise from the microscopic properties of the materials used in constructing the reflector surface. The surface slope errors are measured relative to the ideal surface, and arise from a variety of sources including manufacturing processes and environmental effects such as wind and weight loading of the heliostat.

Each of the components of the overall surface errors were assumed to be normally distributed and independent, giving a cumulative optical error that is also normally distributed with a standard deviation, σ_{opt}, given by

$$\sigma_{opt}^2 = (\sigma_\psi)^2 + (2\sigma_d)^2 \cdot$$

Here σ_ψ and σ_d are the standard deviations of the specularity and surface normal errors, respectively. More details of this description of the optical situation can be found in Ref. 1.

The hemispherical reflectance of the stretched membrane heliostats was assigned a nominal baseline value of 0.89. Based on a structural analysis, and existing reflector materials and heliostat technology, we established nominal baseline values for σ_{opt} of 2.0 mrad for the focused stretched membrane heliostats and 3.46 mrad for the unfocused heliostats. Variations about these values were examined in the sensitivity studies.

Balance of System

The study investigated industrial process heat (IPH) systems with delivery temperatures of 450°C, 750°C, and 1050°C for plant sizes of 75 MW_{th} and 450 MW_{th} (field sizes of approximately 100,000 m^2 and 700,000 m^2). Only single cavity, open aperture receivers coupled to north fields were considered. No storage was considered for any of the cases.

Although the general characteristics of the plant were the same from system to system, the details were optimized (on the basis of their effect on performance) for each combination of plant size, temperature, heliostat type, and heliostat surface quality. The parameters that were optimized included the tower height, the field size and layout, the receiver height and depth, and the aperture dimensions. Cost sensitivities were then based on assumed costs for these performance-optimized systems.

For the system cost tradeoffs a levelized energy cost (LEC) methodology taken from the current Five Year Research and Development Plan for the Solar Thermal Program (3,4) is employed. The cost and economic assumptions are listed in Table 1.

The DELSOL2 computer code (5) was the primary field/receiver modeling tool used in this analysis. DELSOL2 provides an analysis procedure for configuring a central receiver design. It allows the optimization of the system design parameters and permits the prediction of annual system performance.

The receiver radiative losses were calculated using RADSOLVER (6) and SHAPEFACTOR (7). The calculations were performed for a greybody (single band) radiosity model using the solar flux distribution predicted by DELSOL2. The convective losses were calculated using a correlation developed by Kraabel (8). The aperture dimensions were optimized by trading off the spillage (interception) against these thermal losses.

One figure of merit used extensively in this paper

Table 1. Levelized Energy Cost Assumptions

COSTS (all costs in 1984 $/m^2 of heliostat)	
Heliostats	$50 or $100
Receiver	$45
Transport	$25
Balance of plant	$50
Annual O&M	$ 5
Indirects and contingencies[2]	20%
FINANCIAL PARAMETERS	
Discount rate (real)	0.10
Fixed charge rate	0.1334
Capital recovery factor	0.1175
Construction time adjustment factor	1.1033

[2]The total capital cost of the system was calculated by summing the costs for the individual components and increasing that value by 20% to account for indirect costs and contingency factors (4).

to compare the various types of heliostats is the amount of energy delivered by that heliostat. The predicted energy delivered is always reported on an annual basis, per square meter of reflector surface. In many of the figures in the following sections, we normalize the energy delivered by the stretched membrane heliostat systems with the energy delivered by the corresponding baseline, 100-m^2 glass/metal heliostat system. Since this is a common form of presentation in this paper, the resulting ratio will be referred to hereafter as the "normalized annual energy delivery."

RESULTS

Focused Stretched Membrane Heliostats

In this section we describe the system cost and performance for the focused stretched membrane heliostats relative to the 100-m^2, second-generation glass/metal heliostats. For each heliostat parameter examined we first address performance issues and then introduce the cost/performance sensitivities. Although most of the results presented in this section are for the 75-MW_{th} plant size, the trends shown are qualitatively the same for the 450-MW_{th} plant size.

A sense of the performance of the focused stretched membrane heliostats relative to the glass/metal heliostats is given in Figure 1, which shows the normalized annual energy delivery per unit area of heliostat as a function of delivery temperature for both 75-MW_{th} and 450-MW_{th} plant sizes. In each case, the energy delivered by the stretched membrane heliostats has been normalized by the energy delivered by the glass/metal heliostats at the same temperature and plant size.

One of the early conclusions of this study is demonstrated in Figure 1. Over the range of plant sizes and delivery temperatures studied, there is no significant size effect for the focused stretched membrane heliostat. That is, the heliostats with smaller diameters do not perform significantly better than those with larger diameters. This finding was used to simplify our subsequent analysis and comparisons, since it allowed us to consider only the largest (100 m^2) size of focused stretched membrane heliostats.

Figure 2 demonstrates the performance sensitivity of the focused stretched membrane system as the standard deviation of the overall surface error, σ_{opt}, is increased beyond the baseline levels. For the 100-m^2 focused stretched membrane heliostats, Figure 2 shows the normalized annual energy as a function of the

stretched membrane heliostat surface error at several values of the delivery temperature for a 75-MW_{th} plant. The performance shows a significant decrease as the total surface error is increased from the nominal baseline value of σ_{opt} = 2.0 to the highest value of σ_{opt} = 4.80. Note that the high temperature systems are more sensitive to a decrease in the optical quality than the lower temperature systems. Since higher temperature systems have larger thermal losses out of the aperture, the trade-off between thermal losses and spillage tends to produce a smaller aperture than for systems with lower temperatures. This trend to smaller apertures with higher temperatures increases the importance of tighter focusing requirements for the heliostats, and leads to the increased sensitivity shown here.

In Figure 3, the levelized energy cost (LEC) is shown as a function of σ_{opt} for a 75-MW_{th} plant at 750°C and 1050°C. Here two values of stretched membrane (SM) heliostat cost ($50/$m^2$ and $100/$m^2$) are used, and for comparison the LEC assuming the baseline glass/metal (G/M) heliostats (at $100/$m^2$ and 750°C) is also shown. The overall surface error (as measured by σ_{opt}) can be increased nearly 73% relative to the glass/metal value (from 2.0 mrad to 3.414 mrad), and stretched membrane heliostats costing $100/$m^2$ would still be cost-effective. Further, for stretched membrane heliostats costing $50/$m^2$, surface error increases of 240% relative to the glass/metal values (from 2.0 mrad to 4.8 mrad) would still result in lower LEC values for the stretched membrane heliostats.

The relative sensitivity of the annual energy delivery and the LEC to changes in the surface normal, specularity, and reflectivity parameters is shown in Figures 4 and 5 for two delivery temperatures. The abscissa in these plots is the ratio of the value of the independent variable (e.g., σ_d) to its nominal baseline value, while the ordinate shows the ratio of the change in the dependent variable (e.g., LEC) to its nominal value. Thus the slope of the line on the plot indicates the degree of sensitivity of the dependent variable to changes in the independent variable. Both figures show the results for a 75-MW_{th} system using 100-m^2 focused stretched membrane heliostats.

Both figures indicate that the largest sensitivity in the results is to variations in hemispherical reflectivity, where, for example, a 10% reduction in the hemispherical reflectivity can cause a 10% reduction in the performance. The next largest sensitivity is to surface slope errors, and the lowest degree of sensitivity is to the specularity errors. In fact, rather dramatic changes in σ_d and σ_ψ have only small (<10%) changes in E/A and LEC. In addition to these observations we can see that an increase in delivery temperature produces an increase in the sensitivity to the surface and the specularity errors.

Unfocused Stretched Membrane Heliostats

In this section we examine the cost/performance tradeoffs of unfocused stretched membrane heliostats for much the same range of system parameters as used for the focused heliostats. In addition, the unfocused stretched membrane heliostat size is varied from 25 to 100 m^2, and the surface errors, σ_{opt}, are varied from 2 to 3.46 mrad (measured relative to the flat condition).

On first examination, it appears that unfocused stretched membrane heliostats may have a significant economic advantage relative to focused stretched membrane heliostats because of their lower initial and operating costs, particularly since no control mechanism or pumping power is required to maintain the focus. However, they also have the disadvantage of

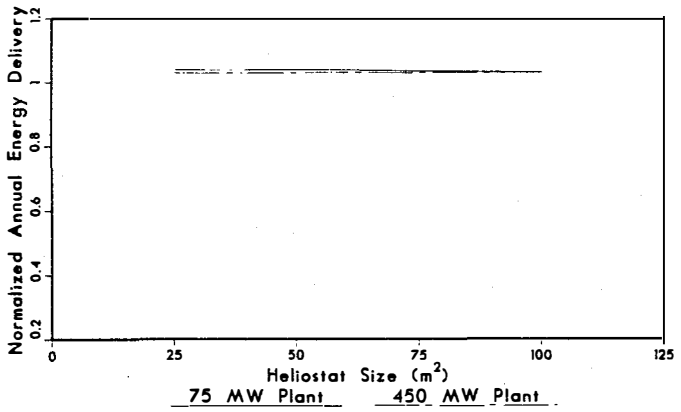

Figure 1. Normalized Annual Energy Delivered as a Function of Focused Stretched Membrane Heliostat Area. Normalized by the 100-m^2 Glass/Metal Focused Heliostat.

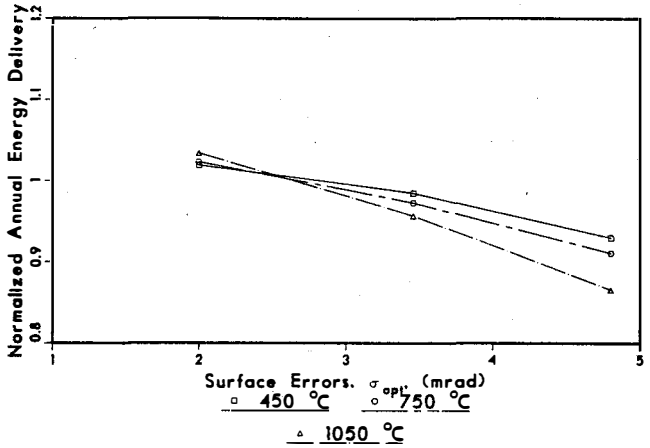

Figure 2. Normalized Annual Energy Delivered by Stretched Membrane Heliostat Systems with Various Levels of Surface Error, Normalized by the Annual Energy Delivered by State-of-the-Art Glass/Metal Heliostat System for a 75-MW_{th} Plant.

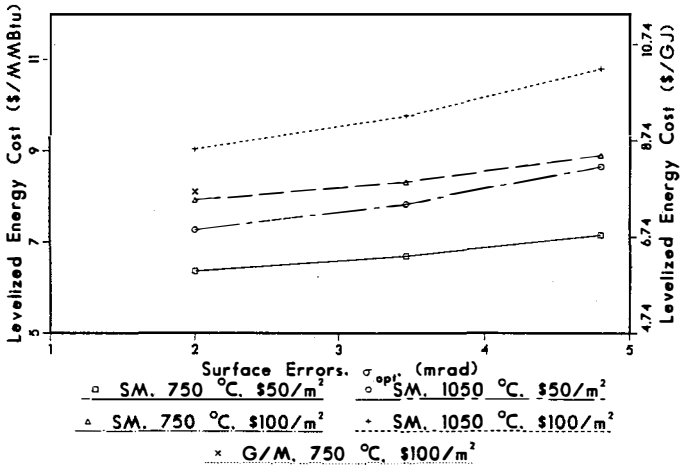

Figure 3. Levelized Annual Energy Cost as a Function of Surface Error for the 75-MW Plant (as in Figure 2).

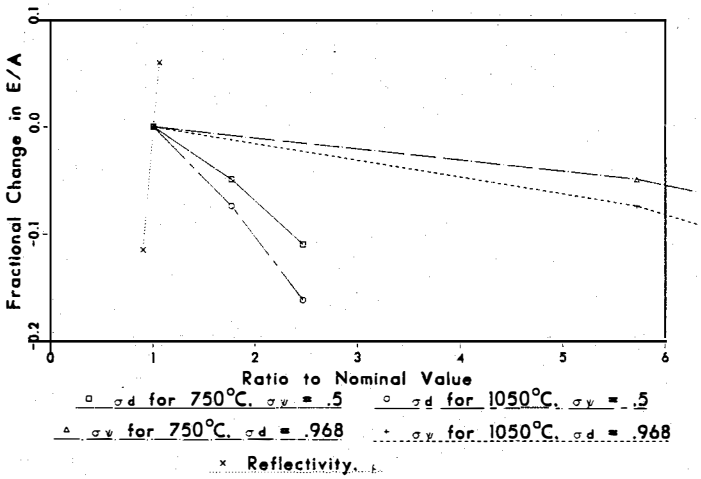

Figure 4. A Comparison of the Relative Effects of Several Optical Parameters on the Annual Energy Delivery for a 75-MW Plant Using Focused Stretched Membrane Heliostats. The ordinate shows the fractional change in the energy delivered relative to the baseline, while the abscissa represents the ratio of the independent parameter to its baseline value. The independent parameters are the surface normal errors, σ_d (assuming σ_ψ = 0.5 mrad), the specularity errors, σ_ψ (assuming σ_d = 0.968 mrad), and the hemispherical reflectivity, ρ.

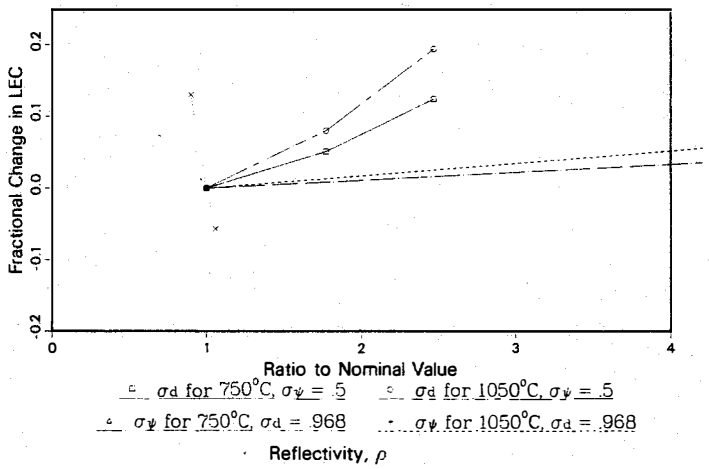

Figure 5. A Comparison of the Relative Effects of Several Optical Parameters on the Levelized Energy Cost for a 75-MW Plant Using $50/m^2 Focused Stretched Membrane Heliostats and the Same Optical Parameters as Figure 4.

poorer optical performance relative to a focused module of the same size. This lower performance is the result of two factors. First, since there is no focusing, the reflected image size will be a strong function of the reflector size. Second, since no control of the surface is assumed, the wind and weight loads will cause the surface to deform relative to its initial state considerably more than the focused modules.

It is demonstrated in Ref. 1 that the value σ_{opt} = 2.0 represents a lower bound on the optical surface error attainable with unfocused and uncontrolled reflector surfaces. This level is most likely to be approached by the small diameter designs. This is because the major contributor to values above σ_{opt} = 2.0 results from axisymmetric deformation, which is proportional to the radius of the design (assuming all other variables are constant). On the other hand, since we have taken no credit for gravity-induced focusing, by careful design one may be able to do noticeably better than the baseline value of σ_{opt} = 3.46 assumed here, even for the large diameter heliostats.

Figure 6 shows the normalized annual energy delivery for unfocused stretched membrane heliostats in both plant sizes as a function of the delivery temperature. The first thing that we can observe is that as the temperature is increased the performance of unfocused stretched membrane heliostats relative to the glass/metal heliostats falls off (i.e., the normalized annual energy decreases). At 450°C even the 100-m^2 unfocused stretched membrane heliostats in a 75-MW$_{th}$ plant can produce nearly 88% as much energy per unit area as the glass/metal heliostats. However, the normalized energy for both sizes of heliostat in the 75-MW$_{th}$ systems (the two bottom curves) decreases markedly with increasing temperature. This decrease in the relative performance occurs because the higher temperature systems have larger thermal losses per unit area of aperture, and thus relatively smaller optimized

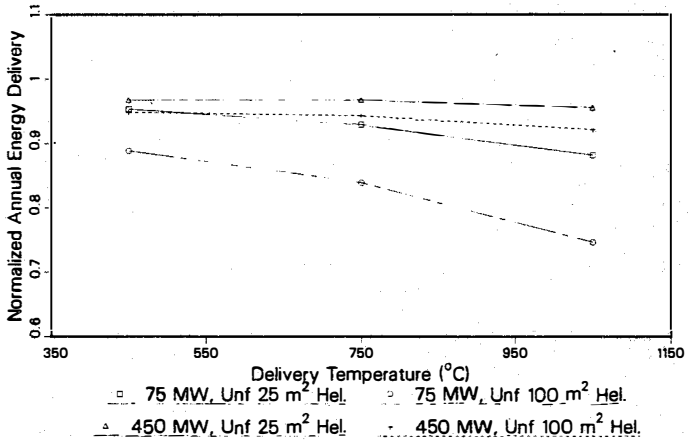

Figure 6. Annual Energy Delivery for Several Stretched Membrane Heliostat Systems Normalized by the Energy Delivered by a Glass/Metal Heliostat System as a Function of the Delivery Temperature.

apertures. Therefore, as the temperature is increased, not only is the required increase in the optimized aperture area a larger fraction of the nominal aperture, but the penalty (in increased thermal losses) for enlarging the aperture size is also increased.

Another notable feature of Figure 6 is the effect of heliostat size. Because of the (nominally) flat nature of the reflector surface, the image size at the receiver aperture is directly related to the diameter of the heliostat. Thus, as the diameter of an unfocused stretched membrane heliostat is reduced the losses caused by lack of focusing are reduced.

The results in Figure 6 also show that smaller system sizes and higher temperatures contribute to increased sensitivity to the heliostat size and the delivery temperature. In particular, we can see that the difference between the two bottom curves (for 75-MW$_{th}$ plant size and 100-m^2 and 25-m^2 heliostat sizes) is much larger than the difference between the corresponding curves for the 450-MW$_{th}$ systems. Similarly, the performance of the two 450-MW$_{th}$ systems is much less sensitive to increasing temperature than the performance of the 75-MW$_{th}$ systems.

The four curves in Figure 6 represent two different heliostat sizes, 25 and 100 m^2, for plant sizes of 75 and 450 MW_{th}. Since they were all generated for a constant value of σ_{opt} = 3.46, this is equivalent to assuming that a decrease in the heliostat size affects only the size error and not the surface errors. In fact, the surface errors will also probably decrease with decreasing heliostat size.

As mentioned above, a good upper bound estimate of the smallest errors likely for a (small) unfocused stretched membrane heliostat is about σ_{opt} = 2.00 mrad. In Figure 7 we can see the effects on the performance of increasing the surface errors. The top curve shows the effect on a focused stretched membrane heliostat, while the three bottom curves are for unfocused heliostats of three sizes. All of the values are for a 75-MW_{th} plant at a 750°C delivery temperature. Notice that although the performance of the unfocused heliostat systems is poorer than the focused system, the sensitivity of the performance to increasing surface errors is nearly identical.

Figures 8 and 9 present a comparison of the relative economics of focused-versus-unfocused stretched membrane heliostats. These plots answer the question "How much more can one afford to pay for focused heliostats without increasing the levelized cost of delivered energy?" The unfocused heliostats were assumed to cost \$50/m^2, and the economic assumptions were taken from the current Solar Thermal Five Year Research and Development Plan (3,4).

In essence, Figures 8 and 9 show that, for the larger surface error cases, unfocused heliostats appear to be advantageous if the cost of focusing exceeds the range from about \$4/m^2 to about \$30/m^2. However, if the surface errors on the unfocused heliostats can be reduced to those of the focused module, the allowable cost of focusing drops significantly, ranging from only several cents per square meter to about \$7/m^2.

One assumption implicit in the analysis behind Figures 8 and 9 is that heliostat cost per square meter is independent of heliostat size. Clearly this assumption ignores the increase in the number of supports, tracking mechanisms, and controls that accompany a decrease in the size of the heliostat. Nonetheless, the results presented should be useful as guidelines as long as the total installed cost per square meter is used in the comparison.

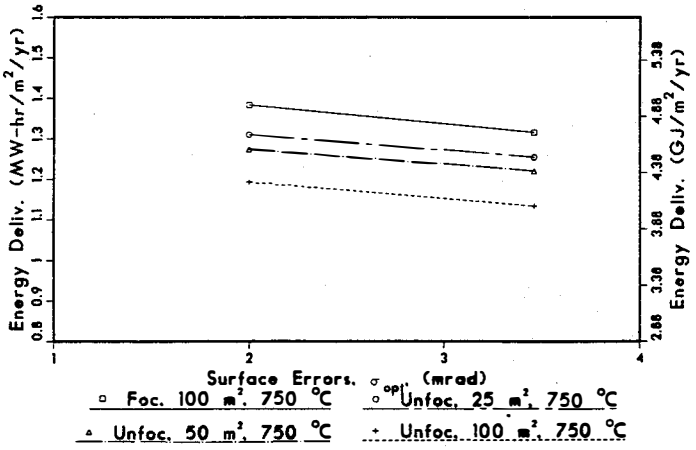

Figure 7. Effect of Surface Errors on the Annual Energy Delivery for Several Sizes of Unfocused Stretched Membrane Heliostats in a 75-MW Plant at 750°C Delivery Temperature. The effect of the surface errors on focused stretched membrane heliostats is included for comparison.

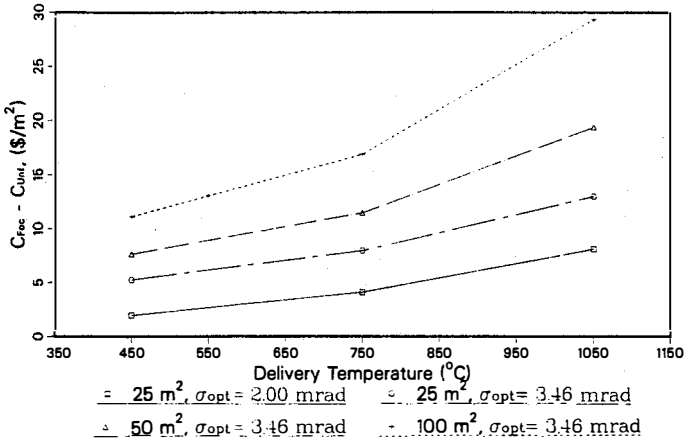

Figure 8. Allowable Cost of Focusing as a Function of Delivery Temperature for a 75-MW Plant.

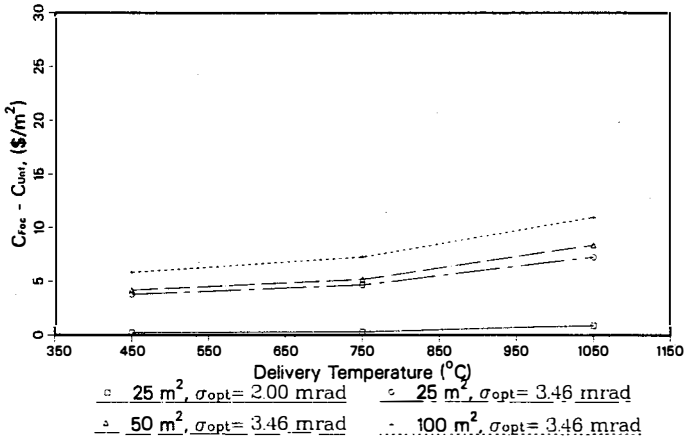

Figure 9. Allowable Cost of Focusing as a Function of Delivery Temperature for a 450-MW Plant.

CONCLUSIONS

Based on the ground rules and assumptions, the major findings of this study are listed below.

Focused Stretched Membrane Heliostats

Overall, focused stretched membrane heliostats appear to have the potential to perform at levels that are quite close to glass/metal heliostats. However, to achieve this parity in performance it is important that the optical quality--in particular, the hemispherical reflectivity and the macroscopic surface errors introduced in manufacturing--be comparable to the glass/metal heliostats.

The performance of focused stretched membrane heliostats appears to have the same sensitivity to variations in optical quality parameters as the performance of glass/metal heliostats. In addition, the performance of the focused stretched membrane heliostats is nearly independent of heliostat size for the plant sizes studied.

Unfocused Stretched Membrane Heliostats

Heliostat diameter is a very important parameter when considering unfocused stretched membrane heliostats because: the size of the image at the receiver is strongly dependent on the heliostat size for the unfocused modules. In addition,it appears that it will be possible to achieve smaller surface normal errors with smaller diameter heliostats.

In terms of their performance, unfocused heliostats become relatively more attractive at lower temperatures, larger system sizes, and for smaller heliostat module sizes.

General Considerations

In general, the sensitivity of the performance of central receiver systems to poorer optical quality in the heliostats tends to increase with higher temperatures and smaller plant sizes.

Overall, the unfocused stretched membrane heliostats demonstrate a remarkable level of performance, competing quite closely with both the focused stretched membrane heliostats and the glass/metal heliostats over an impressive range of system parameters. However, focusing does seem quite desirable if a single heliostat design is to have the largest range of applicability. Based on the performance analyses, focusing is especially beneficial for small plant sizes and high temperatures. However, as the plant size increases and/or the temperature decreases the benefit of focusing diminishes.

For the baseline assumptions we found that the sensitivity of system performance to variations in specularity errors was much less than that corresponding to variations in either hemispherical reflectivity or surface normal errors. For the range of systems studied, the specularity half-cone angle that includes 90% of the reflected energy can be as large as about 6 mrad (from a baseline of 1 mrad) while producing a less than 5% decrease in annual system performance.

REFERENCES

1. Murphy, L. M. et al., "System Performance and Cost Sensitivity Comparisons of Stretched Membrane Heliostat Reflectors with Current Generation Glass/Metal Concepts," SERI/TR-253-2694, Solar Energy Research Institute, Golden, CO, April 1985.

2. Pettit, R. B., C. N. Vittitoe, and F. Biggs, "Simplified Calculational Procedure for Determining the Amount of Intercepted Sunlight in an Imaging Solar Concentrator," Journal of Solar Energy Engineering, Vol. 105, Feb. 1983.

3. Sandia National Laboratories, "National Solar Thermal Technology Program - Draft Five Year Research and Development Plan 1985-1989," Livermore, CA, Dec. 1985.
See also Williams, T. A., "Long-Term Performance and Cost Goals for Solar Thermal Technology," Proceedings of the ASME Winter Annual Meeting, Nov. 17-22, 1985.

4. Williams, T. A., Personal Communication. This factor is necessary to calculate levelized energy costs that are comparable to the cost goals published in Ref. 3.

5. Dellin, T. A. et al., "A User's Manual for DELSOL2: A Computer Code for Calculating the Optical Performance and Optimal System Design for Solar Thermal Central Receiver Plants," SAND81-8237, Sandia National Laboratories, Aug. 1981.

6. Abrams, M., "RADSOLVER - A Computer Program for Calculating Spectrally Dependent Radiative Heat Transfer in Solar Cavity Receivers," SAND81-8248, Sandia National Laboratories, Oct. 1980.

7. Emery, A. F., "Instructional Manual for the Program SHAPEFACTOR," SAND80-8027, Sandia National Laboratories, Oct. 1980.

8. Siebers, D. L. and J. S. Kraabel, "Estimating Convective Energy Losses from Solar Central Receivers," Sandia National Laboratories, SAND84-8717, April 1984.